Inhibition of Prostate Cancer Growth by Muscadine Grape Skin Extract and Resveratrol through Distinct Mechanisms

Tamaro S. Hudson,[1] Diane K. Hartle,[2] Stephen D. Hursting,[3] Nomeli P. Nunez,[3] Thomas T.Y. Wang,[4] Heather A. Young,[5] Praveen Arany,[1] and Jeffrey E. Green[1]

[1]Laboratory of Cellular Regulation and Carcinogenesis, National Cancer Institute, NIH, Bethesda, Maryland; [2]College of Pharmacy, Department of Pharmaceutical and Biomedical Sciences, University of Georgia, Athens, Georgia; [3]Division of Nutritional Sciences, University of Texas, Austin, Texas; [4]Phytonutrients Laboratory, Beltsville Human Nutrition Research Center, U.S. Department of Agriculture, Beltsville, Maryland; and [5]Department of Epidemiology and Biostatistics, The George Washington University School of Public Health and Health Services, Washington, District of Columbia

Abstract

The phytochemical resveratrol contained in red grapes has been shown to inhibit prostate cancer cell growth, in part, through its antioxidant activity. Muscadine grapes contain unique phytochemical constituents compared with other grapes and are potentially a source for novel compounds with antitumor activities. We compared the antitumor activities of muscadine grape skin extract (MSKE), which we show contains no resveratrol, with that of resveratrol using primary cultures of normal prostate epithelial cells (PrEC) and the prostate cancer cell lines RWPE-1, WPE1-NA22, WPE1-NB14, and WPE1-NB26, representing different stages of prostate cancer progression. MSKE significantly inhibited tumor cell growth in all transformed prostate cancer cell lines but not PrEC cells. Prostate tumor cell lines, but not PrEC cells, exhibited high rates of apoptosis in response to MSKE through targeting of the phosphatidylinositol 3-kinase–Akt and mitogen-activated protein kinase survival pathways. The reduction in Akt activity by MSKE is mediated through a reduction in _Akt_ transcription, enhanced proteosome degradation of Akt, and altered levels of DJ-1, a known regulator of PTEN. In contrast to MSKE, resveratrol did not induce apoptosis in this model but arrested cells at the G_1-S phase transition of the cell cycle associated with increased expression of p21 and decreased expression of cyclin D1 and cyclin-dependent kinase 4 proteins. These results show that MSKE and resveratrol target distinct pathways to inhibit prostate cancer cell growth in this system and that the unique properties of MSKE suggest that it may be an important source for further development of chemopreventive or therapeutic agents against prostate cancer. [Cancer Res 2007;67(17):8396–405]

Introduction

Epidemiologic evidence strongly suggests that a diet rich in fruits and vegetables is associated with a reduced risk of developing many types of cancers, including prostate cancer (1). Because such diets are rich sources of phytochemicals, it has been suggested that the relatively low risk of developing prostate cancer among Asian men may be attributed in part to the high consumption of phytochemicals (2, 3). Therefore, a more complete understanding of the molecular mechanisms, through which phytochemicals act on cellular processes involved in prostate cancer progression, could lead to improved use of such compounds for the prevention or treatment of prostate cancer.

Resveratrol, a phytoalexin produced in a wide variety of plants (including grapes, peanuts, and mulberries) in response to stress, injury, UV irradiation, and fungal infection (4), has been shown to inhibit growth of several types of cancer. For instance, resveratrol inhibits the growth of MDA-MB-231 breast cancer cells (5), the pancreatic cancer cell lines PANC-1 and AsPC-1, and Caco-2, a colon cancer cell line (6). Hsieh and Wu showed that resveratrol inhibited growth and the G_1-S cell cycle transition in LNCaP, DU-145, and PC-3 cells, increased apoptosis, and lowered both intracellular and secreted prostate specific antigen without affecting the expression of androgen receptor in the LNCaP prostate cells (7). These studies support the concept of developing phytochemicals for anticancer applications.

Muscadine grape (_Vitis rotundifolia_) is a type of grape distinct from the more common red grapes used to produce red wines, a major source of resveratrol. Muscadine grapes are native to Southeastern United States and can be found growing wild from Delaware to the Gulf of Mexico and westward from Missouri to Texas (8). Interestingly, the phytochemical constituents of muscadine grapes differ from most other grape varieties in that they contain a predominance of anthocyanin 3,5-diglucosides, ellagic acid, and ellagic acid precursors (9). Anthocyanins produce the red and purple colors of the grapes, have strong antioxidant activity (10), and show antitumor activities by blocking carcinogen-induced DNA adduct formation (11), inhibiting DNA synthesis in breast cancer cells (12), and retarding blood vessel growth in some tumors (13). Moreover, aqueous extracts of the whole muscadine berry have been shown to inhibit the activities of matrix metalloproteinases (MMP2 and MMP9), enzymes involved in tumor metastases (14). Importantly, no known toxicities that have been reported to date are related to products of muscadine grapes. Although these previous studies suggest that anthocyanins, which are constituents of the muscadine grape, may suppress tumorigenesis, the mechanisms underlying these effects have not been well elucidated.

In this study, we show that muscadine grape skin extract (MSKE) does not contain significant amounts of resveratrol and that the major components of MSKE are different from those in muscadine grape seed extract (MSEE), which has also been studied for antitumor activities (15). Using a well-characterized series of transformed human prostate cancer epithelial cell lines that

represent different stages of prostate cancer progression (16), we show that MSKE significantly inhibits growth of transformed, but not normal, prostate cells, primarily through the induction of apoptosis by down-regulating the phosphatidylinositol 3-kinase (PI3K)–Akt survival pathway. In contrast, resveratrol seems to act in this system by inducing cell cycle arrest through modulation of the cell cycle regulators p21, cyclin-dependent kinase 4 (Cdk4), and cyclin D1. These results show that MSKE has potent proapoptotic antitumor activities that differ from the effects of resveratrol shown in this system, suggesting that MSKE warrants further development as a potential chemopreventive or therapeutic agent.

Materials and Methods

Chemicals and preparation of MSKE. Resveratrol, DMSO, propidium iodide, and Z-leu-leu-leu-al (MG132 proteosome degradation inhibitor) were purchased from the Sigma Chemical. Dried and pulverized muscadine grape skin was obtained from Muscadine Products Corporation. The muscadine skin powder was prepared from the *Ison cultivar,* a purple-skinned variety. Similarly, dried and ground muscadine ground seeds from the Ison variety were used for the muscadine seed extract. A single, large preparation of MSKE was used for all experiments in this study. Polyphenolic compounds from the dried and pulverized muscadine grape skin were extracted with 50% ethanol/water at a nominal ratio of 9:1 (v/w) by stirring with a magnetic stir bar for 1 h at room temperature. The slurry was allowed to settle for 24 h, and the supernatant was passed through a 0.2 μmol/L membrane filter funnel (Nalgene) and collected under a vacuum.

Reagents. The antibodies used in this study were as follows: Akt, phosphorylated Akt, phosphorylated GSK-3β, phosphorylated FKHR, phosphorylated PDK1, PI3K-p85, phosphorylated extracellular signal-regulated kinase (ERK), ERK, phosphorylated p38, p38 (all from Cell Signaling), androgen receptor, p21, p27 (all from Santa Cruz), cyclin D1, Cdk2 (Clone 2B6), Cdk4 (Clone DCs-35), cyclin E (Clone HE12; all from NeoMarkers), actin (Chemicon), DJ-1 (Stressgen KAM-SA100).

Culture of human prostate epithelial cell lines. The development of the cell lines RWPE-1 and its *N*-methyl-*N*-nitrosourea–derived cell lines (WPE1-NA22, WPE1-NB14, and WPE1-NB26) were originally described by the laboratory of Muktar Webber (16). The RWPE-1 cell line was immortalized by human papillomavirus 18, and sublines were further transformed with *N*-methyl-*N*-nitrosourea to produce the additional lineages of prostate tumor cell lines: RWPE-1 is nontumorigenic when injected into mice; WPE1-NA22 cells form tumors with a relatively low growth rate; WPE1-NB14 cells are highly tumorigenic but not highly metastatic; and WPE1-NB26 cells are highly metastatic. Cells were cultured in complete KSFM containing 50 μg/mL bovine pituitary extract (BPE), 5 ng/mL epidermal growth factor (EGF), and 1% antibiotics (penicillin 100 units/mL, streptomycin 100 μg/mL; Invitrogen). PrEC normal prostate cells were grown according to the manufacturer's directions in PrEGM medium (Clonetics). LnCaP and Du-145 prostate cancer cell lines were grown as previously described. Cells were passaged using trypsin/EDTA and trypsin neutralizing solution (Clonetics). Cultured cells were maintained in a humidified incubator containing 5% CO_2 at 37°C. The cells were viewed using a Zeiss Axiovert 200 microscope (Zeiss) using Spot Basic imaging software.

Recovery of transresveratrol by high-pressure liquid chromatography analysis. To exclude the possibility that MSKE contained significant amounts of resveratrol, the amount of resveratrol contained in MSKE was determined and compared with that of MSEE. Extracts were prepared as described above. But after ethanol extraction, the slurry was allowed to settle and the supernatant was decanted off into a Buchner filter funnel containing a glass fiber filter. The filtrate was collected under vacuum followed by a second filtration through a cellulose fiber filter. Before analysis, an aliquot of extract was passed through a 0.45-μm nylon membrane filter using a syringe, then dried using vacuum centrifugation. The resulting residue was redissolved in 10% acetonitrile/water. Extracts were stored at 4°C.

Analysis was carried out using an Agilent Technologies series 1100 Capillary LC/MSD-Trap equipped with a binary pump, online degasser, diode array UV detector with 500-nL flow cell, thermostated micro-autosampler, and ion trap mass spectrometer. Separation was accomplished by reversed-phase chromatography using a 150 mm × 0.5 mm ID microcolumn packed with 5-μm Beta-Basic C18 stationary phase obtained from Thermo. The mobile phase used was composed of 0.1% formic acid in water and 0.1% formic acid in acetonitrile delivered at 25 μL/min as a linear gradient from 10% acetonitrile for 1 min, increased to 50% over 19 min and then increased to 80% over 5 min for a total runtime of 25 min. Autosampler variables included an injection volume of 5 μL and a sample tray temperature of 4°C. The UV detector was set to monitor the λ_{max} for transresveratrol at 306 nm to provide maximum sensitivity for quantification. Peak identity was confirmed using mass spectrometric detection of the deprotonated molecular ion at 227.1 m/z. The MS was operated in negative ion mode using electrospray ionization.

Resveratrol was identified by comparing the retention time of the standard compound to the sample and by correlation to the extracted ion chromatogram for 227.1 m/z from the mass spectrometry signal output. Resveratrol (5 μg/mL) was also added to MSKE as a positive control, and the sample peak was acquired under the same high-pressure liquid chromatography (HPLC) conditions as mentioned above. Quantification was accomplished by applying the peak area from the sample chromatogram obtained from UV detection to a calibration curve generated using standard solutions from 0.1 to 50 μg/mL. The limit of quantification was equivalent to 1 μg/g dry weight of skin or seed.

Proliferation assay. PrEC, RWPE-1, and its *N*-methyl-*N*-nitrosourea–derived prostate cancer cell lines were plated in quadruplicates at a density of 1×10^4 (100 μL/well) into 96-well plates and incubated for 24 h in two independent experiments. Cells were starved for 24 h (without EGF and BPE), after which resveratrol (0, 5, 10, and 25 μmol/L) or MSKE (0, 2, 5, 10, 20 μg/mL) was given daily. Cells were then harvested at 24, 48, and 72 h. Stock solutions of resveratrol were prepared in DMSO, and MSKE was prepared in 50% ETOH. Equal volumes of DMSO and ETOH (final concentrations, <0.01%) were added to the control cells. Cell viability was measured using MTS [3-(4,5-dimethylthiazol-2-yl)-5-(3-carboxymethoxy-phenyl)-2-(4-sulfophenyl)-2H-tetrazolium, inner salt] cell proliferation assay kit (Promega). Sample absorption (indicative of formazan formation) was determined using an ELISA plate reader (OPTImax microplate reader, MTX Labsystems) at 490 nm. Results are expressed as mean absorbance ± SE.

Fluorescence-activated cell sorting analysis. PrEC, RWPE-1, and its *N*-methyl-*N*-nitrosourea–derived prostate cancer cell lines were plated in duplicates at a density of 1×10^5 cells per well in 6 well plates, which were incubated for 24 h and subsequently synchronized by culturing without EGF and BPE for 24 h in two independent experiments. Based on the results from the cell growth assays, the cells were then treated with resveratrol or MSKE at 25 μmol/L and 20 μg/mL, respectively, for 24 h. The cells were then washed with PBS (Invitrogen), harvested, fixed with 80% ETOH, stained with propidium iodide, analyzed by flow cytometry (FACS Calibur), and evaluated using Cell Quest and ModFit cell cycle analysis software (BD Biosciences).

Apoptosis assays. Cells were plated in duplicate at a density of 1×10^5 cells per well in six-well plates in complete keratinocyte serum–free medium for 24 h and/or 48 h. Subsequently, EGF and BPE were removed from the media for 24 h, after which time media containing EGF and BPE was provided to the cells with or without resveratrol or MSKE. The cells were harvested, washed with PBS, stained using the Annexin V–FITC antibody detection kit according to the manufacturer's protocol (BD Biosciences), and analyzed by fluorescence-activated cell sorting (FACS). The data was evaluated using Cell Quest analysis software. Results are expressed as mean percentage ± SE for two separate experiments. For *in situ* apoptosis analysis, TUNEL staining was done (Roche Applied Sciences). RWPE-1 and the *N*-methyl-*N*-nitrosourea–derived prostate cancer cell lines were plated at a density of 4×10^4 cells per well in an eight-chamber slide platform (Nunc-labtek, Nunc) in complete kertinocyte serum–free medium for 24 h and subsequently growth factor–starved for 24 h. Cells were then treated with or without 20 μg/mL MSKE for 24 h.

The cells were then washed twice with PBS and allowed to briefly dry. The TUNEL reaction fluorescence mixture was added according to the manufacturer's directions (Roche Applied Sciences) to each well and placed in a humidified incubator for 1 h at 37°C. Subsequently, cells were washed thrice with PBS and then analyzed under a fluorescence microscope.

Signal transduction phosphorylation analyses. The human phosphorylated mitogen-activated protein kinase (MAPK) array kit was used according to manufacturer's protocol (R&D Systems). WPE1-NB26 metastatic prostate cells were plated at a density of 6×10^5 cells in a 10-cm dish in complete keratinocyte serum–free medium for 24 h, starved without growth factors for 24 h, and then treated with or without 20 μg/mL MSKE for 4 or 8 h. The cells were rinsed with cold PBS and lysed according to the manufacturer's protocol. The lysate (250 μg) was added to the nitrocellulose membrane array, which was incubated overnight at 2°C to 8°C on a rocker platform, washed, and incubated with the detection antibody cocktail. After washing, secondary antibody (streptavidin–horseradish peroxidase, 1:2,000) was added. Protein signals were detected by the enhanced chemiluminescence system. Western analysis was done on total cell lysates. Duplicate gene signals on the array were quantitated using AlphaEase Fluorochem imaging software (IMGEN Technologies). Results are expressed as average pixel density ± SE.

Protein isolation and Western blotting. Cells were cultured as described above for 0, 30 min, 8 h, and/or 24 h, washed with cold PBS, and then lysed with cell lysis buffer (17) containing 25 mmol/L HEPES (pH 7.5), 100 mmol/L NaCl, 10% glycerol, 5 mmol/L EDTA, and 1% Triton X-100 supplemented with protease inhibitors (Roche Applied Sciences), 50 mmol/L sodium fluoride, and 1 mmol/L sodium orthovandate. Proteins (20 μg) were separated using 10% or 16% precast Tris-glycine gels and transferred overnight onto nitrocellulose membranes (Invitrogen). The membrane was blocked for 1 h with 3% bovine serum albumin (BSA) in TBST [15 mmol/L NaCl/100 mmol/L Tris (pH 7.5)/0.1% Tween] and probed with anti–DJ-1 (1:1,000 diluted in 1% BSA in TBST), PI3K-p85, phosphorylated PDK1, AKT, phosphorylated Akt, ERK, phosphorylated ERK, p38, phosphorylated p38, phosphorylated GSK-3β, cyclinD1 (1:500 diluted in 1% BSA in TBST), or androgen receptor (1:200 diluted in 1% BSA in TBST) overnight at 4°C. After washing with TBST, the blots were treated with horseradish peroxidase–conjugated antibody for 20 min and washed several times. Proteins were detected by the enhanced chemiluminescence system. Western analysis was done on total cell lysate.

For the proteosome degradation Western assay, the above protocol was followed except that the WPE1-NB26 prostate cells were treated with or without 20 μg/mL MSKE, 20 μmol/L MG132, proteosomal degradation inhibitor plus 20 μg/mL MSKE for 0, 4, and/or 8 h. The blot was probed with anti–PI3K-p85 and Akt.

To evaluate the effects of resveratrol on protein expression of cell cycle regulators, the above protocol was followed, except that all four cell lines were treated with 25 μmol/L resveratrol for 24 h. The blot was probed with anti-cdk4, cyclin D1, cdk2, cyclin E, p21, and p27.

Real-time PCR. Total RNA was extracted using Trizol (Invitrogen). cDNA (3 μg) was prepared using the SuperScript First-Strand Synthesis System for reverse transcription-PCR kit (Invitrogen) according to the manufacturer's protocol. The PCR reactions were done using the SYBR green QPCR master mix (Stratagene) according to the manufacturer's instructions. Before the PCR reaction, a dilution series and standard curve were generated for glyceraldehyde-3-phosphate dehydrogenase (GADPH) and each target gene from the untreated and treated prostate cancer sample cDNAs (Applied Biosystems). Quantitative PCR was done with a polymerase-activating step of 95°C for 10 min, followed by 40 cycles of a cycling program of 95°C for 15 s and 60°C for 1 min with a dissociation curve program of 95°C for 15 s, 60°C for 1 min, and 95°C for 15 s in an ABI Prism 7500 sequence detector (Applied Biosystems). Forward and reverse primers were respectively as follows: human *Akt1*, 5′-ATGAGCGACGTGGC-TATTGTGAAG-3′ and 5′-GAGGCCGTCAAGCCCACAGTCTGGATG-3′; human *Akt2*, 5′-ATGAATGAGGTGTCTGTCATCAAAGAAGGC-3′ and 5′-TGCTTGA-GGCTGTTGGCGACC-3′; human *Akt3*, 5′-ATGAGCGATGTTACCATTGT-3′ and 5′-CAGTCTGTCTGCTACAGCCTGGATA-3′ (18); human *DJ-1*, 5′-GGAGA-CGGTCATCCCTGTAGAT-3′ and 5′-GCTACACTGTACTGGGTCTTTTCCA-3′

(19); human GADPH, 5′-TGCACCACCAACTGCTTAGC-3′ and 5′-GGCATG-GACTGTGGTCATGAG-3′. The relative expression levels of each gene were calculated by dividing the expression level of *Akt1, Akt2, Akt3,* and *DJ-1* by the expression level of *GADPH* for each sample and compared with the untreated corresponding control. Quantitative analysis of gene expression was done using the $2^{-\Delta\Delta C_T}$ method.

Statistical analysis. All statistical procedures were carried out using SAS Institute Inc. version 8 statistical software package (SAS Institute). Statistical analysis evaluating cellular proliferation and induction of apoptosis used ANOVA followed by Student-Neuman-Keuls post hoc test. To evaluate protein expression levels in the array, we used Student's t test with post hoc Bonferroni adjustments.

Results

MSKE does not contain significant quantities of resveratrol and differs from MSEE. To determine whether MSKE contains significant levels of resveratrol and to compare the chemical content of MSKE (skin) with MSEE (seed), HPLC analyses were done. As depicted in Supplementary Fig. S1*A* and *B*, MSKE does not contain significant amounts of resveratrol (<1 μg/g by limit of detection). However, when resveratrol was added to MSKE as a control, it was readily detected, and 86% of the resveratrol was recovered (data not shown). As seen in Supplementary Fig. S1*B* and *C*, MSKE and MSEE exhibit very different chromatogram patterns indicating that the chemical components in each extract are quite varied with relatively little overlap.

Resveratrol and MSKE alter cellular morphology, inhibit growth, but do not induce senescence of prostate cancer cells. The morphologic changes observed in the normal and transformed human prostate cell lines in response to resveratrol or MSKE are depicted in Supplementary Fig. S2. MSKE-treated cells display condensed nuclei, cell detachment, and irregular shape compared with the control cells after 24 h, consistent with changes occurring during apoptosis. These morphologic changes were seen only in the transformed human prostate cell lines and not in the normal primary PrEC cells. Reservatrol did not induce these changes. However, resveratrol induced morphologic changes after 72 h (data not shown). In addition, neither MSKE nor resveratrol induced senescence in the transformed cells as assessed using the senescence-associated β-galactosidase activity (data not shown).

The effects of different concentrations of resveratrol and MSKE on growth of the prostate cell lines are depicted in Figs. 1*B-D* and 2*B-D*. Resveratrol (25 μmol/L) significantly inhibits cell growth by 72 h in all four transformed human prostate cell lines. Similarly, 5, 10, and 20 μg/mL MSKE significantly inhibited cell growth by at least 50% in the WPE1-NA22, WPE1-NB14, and WPE1-NB26 cell lines by 24 h, with growth inhibition sustained over 72 h. These findings were confirmed using a titrated thymidine proliferation assay (data not shown). Moreover, we observed a similar significant growth inhibition by MSKE in other well-established prostate cancer cell lines, LNCaP and DU-145 (Supplementary Fig. S4). However, in contrast to the reduction in proliferation observed for the prostate cancer cell lines, resveratrol and MSKE did not significantly inhibit cell growth of normal primary prostate cells (Figs. 1*A* and 2*A*). The inhibitory effects were shown to be due to the compound and not the solvents, because solvent alone did not produce growth inhibition and similar inhibitory effects were observed when either ethanol or DMSO were used as solvents.

Resveratrol induces cell cycle arrest in prostate cells through increased expression of p21 and decreased expression of cyclins and cdks. To determine whether the reduction in cell
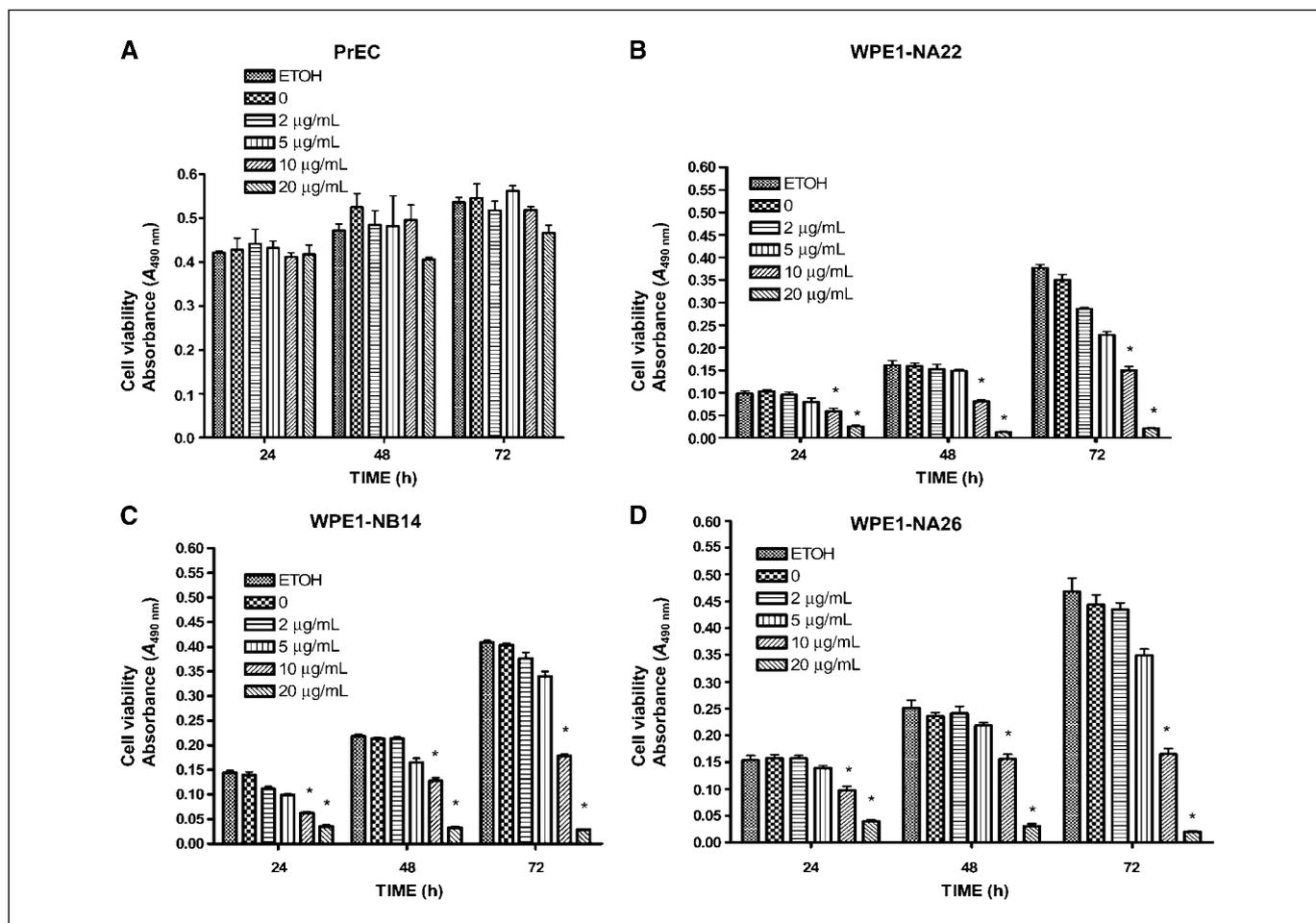
Figure 1. MSKE inhibits cell growth in prostate cancer cells but not normal cells. The effect of MSKE on the growth rate by MTS assay in PrEC normal cells (*A*), WPE1-NA22 premalignant cells (*B*), WPE1-NB14 malignant cells (*C*), WPE1-NB26 metastatic cells (*D*). Cells were plated at a density of 1×10^4 per well for 24 h, starved for 24 h, and treated with MSKE at 24, 48, and 72 h. Subsequently, cells were treated with MTS for 1 h, measured at 490 nm, and plotted. *Columns,* mean absorbance; *bars,* SE. *, significant difference between MSKE treatment and ETOH and untreated control. Significant at $P < 0.05$.

proliferation was due to cell cycle arrest, cell death, or a combination of both, propidium iodide FACS analyses were done. These results reveal that resveratrol blocks the G_1-S phase transition in all four prostate cancer cell lines, whereas MSKE seems to preferentially induce apoptosis. As depicted in Fig. 3*B*, ∼25% more cells from all four transformed cell lines remained in the G_1-S phase of the cell cycle when treated with 25 μmol/L resveratrol compared with the control cells, whereas resveratrol did not significantly inhibit cell cycle progression in normal primary PrEC cells. In contrast, MSKE significantly arrested at least 50% of the transformed prostate cells at the G_0-G_1-S transition and MSKE (Fig. 3*A*) resulted in a 15% increase in cells inhibited at the S-G_2M transition phase compared with the control cells (Fig. 3*B*). However, MSKE does not significantly inhibit cell cycle progression of the primary normal cells.

Based upon the demonstration that resveratrol treatment primarily induced cell cycle arrest at the G_1-S phase transition, the effects of resveratrol on cell cycle regulators of the G_1 phase of the cell cycle were investigated. Immunoblot analysis revealed that treatment with 25 μmol/L resveratrol resulted in a marked reduction of cdk4 and cyclin D1 in all four cell lines (Fig. 6*D*). Decreases in cyclin E protein expression were observed only in RWPE-1, WPE1-NB14, WPE1-NB26 prostate cells. Resveratrol did

not modulate cdk2 protein expression in this system. A marked induction of the major cell cycle inhibitory proteins was also observed in response to resveratrol. p21 was significantly elevated in all four prostate cell lines and p27 was elevated in WPE1-NA22 and WPE1-NB26 at 24 h (Fig. 6*D*).

MSKE, but not resveratrol, induces apoptosis in prostate cancer cells through inhibition of the Akt survival pathway. Based upon both the morphologic and FACS analyses suggesting that MSKE induced apoptosis, additional apoptosis assays were done. The results from the Annexin V–FITC (Fig. 4*A* and *B*) and TUNEL-FITC assays (data not shown) confirm that MSKE, but not resveratrol, induces apoptosis in the transformed prostate cancer cell lines. In addition, a dose-dependent induction of apoptosis was observed in the WPE1-NB26 metastatic cells (Fig. 4*C*), whereas the MSKE did not significantly induce apoptosis in normal primary prostate cells (Fig. 4*D*).

Several studies have shown the critical roles that the signaling pathways related to Akt kinase and MAPK play in regulating cell growth, survival, and inhibition of apoptosis in prostate cancer (20–22). Using a human phosphorylated MAPK protein array that includes major families of MAPK as well as intracellular kinases, such as Akt, GSK-3β, and p70 S6 that are important in signal transduction and cellular proliferation, multiple changes in

phosphorylation states were observed in response to MSKE. MSKE significantly increases phosphorylation by at least 2-fold of targeted c-Jun-NH$_2$-kinase (JNK1, JNK2), p38 isoforms (p38γ, p38α), and intracellular kinases (GSK-3β, MSK2, p70 S6) in WPE1-NB26 metastatic prostate cells after 4 h (Fig. 5*A* and *C*). Similar results were also observed at 8 h with increases in JNK2, p38 isoforms (p38γ, p38α), and intracellular kinases (MSK2). Additionally, as depicted in Fig. 5*B* and *C*, decreases in several intracellular kinases (ERK1, RSK1, Akt1, ERK2, GSK-3β, Akt3) were observed.

Western blot analyses were done to confirm these results. As shown in Fig. 6*A*, 20 µg/mL MSKE treatment of WPE1-NA22 and WPE1-NB26 prostate cell lines resulted in a marked reduction of PI3K p85, phosphorylated PDK1, all three isoforms of Akt, phosphorylated Akt (Thr^{308}), phosphorylated ERK, phosphorylated p38, phosphorylated GSK-3β (Ser^9), cyclin D1, and androgen receptor. In addition, MSKE decreased phosphorylation of Fork-head (FKHR) protein, a downstream effector molecule of the Akt pathway that is involved in caspase activation and induction of apoptosis when dephosphorylated. The decreased expression of PI3K p85, phosphorylated PDK1, Akt, phosphorylated Akt, GSK-3β,

FKHR, cyclin D1, and androgen receptor was observed for 24 h in all transformed prostate cell lines treated with MSKE (Fig. 6*B*). Interestingly, MSKE did not affect total protein levels of p38 and ERK1/ERK2 in WPE1-NA22 and WPE1-NB26 prostate cancer cells. Although, the Akt protein levels were decreased, levels of DJ-1, a novel protein regulator of PTEN, were not altered after 30 min or 8 h (Fig. 6*A*). However, a marked reduction in DJ-1 was observed in the WPE1-NA22, WPE1-NB14, and WPE1-NB26 prostate cancer cell lines at 24 h (Fig. 6*B*). In contrast, Akt protein levels were not altered in cells treated with 25 µmol/L resveratrol (data not shown).

MSKE accelerates degradation of Akt protein. Based upon the above results demonstrating that MSKE significantly suppresses Akt protein expression, we determined whether MSKE alters rates of Akt protein degradation. MSKE was shown to induce Akt protein degradation by 8 h, but not at 4 h (Fig. 6*C*). However, upon coadministration of MGE132, a 26S proteosomal degradation inhibitor, Akt protein levels were maintained in the presence of MSKE, thus suggesting that MSKE accelerates the degradation of Akt protein (Fig. 6*C*).
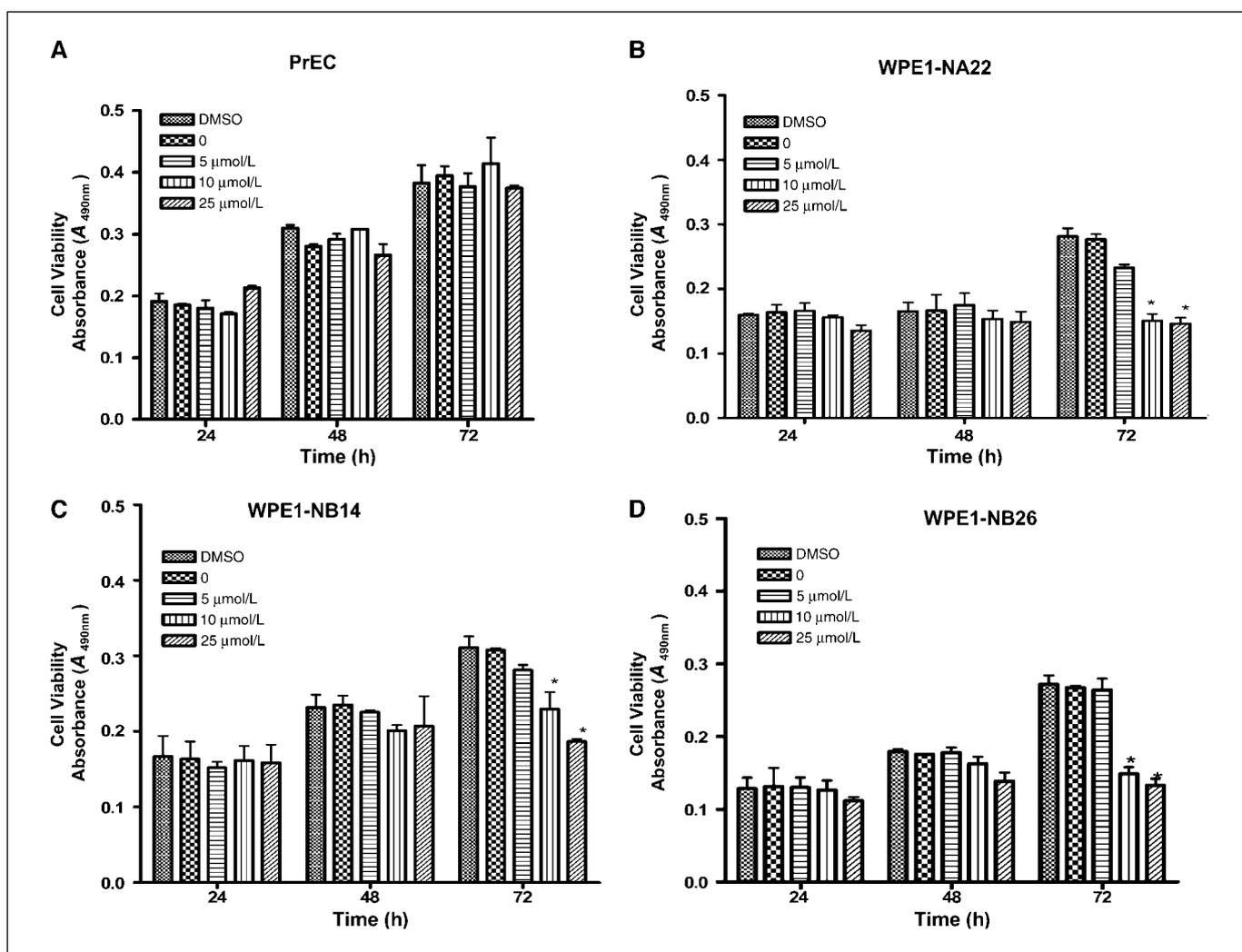

Figure 2. Resveratrol inhibits cell growth in prostate cancer cells but not normal cells. The effect of resveratrol on the growth rate by MTS in PrEC normal cells (*A*), WPE1-NA22 premalignant cells (*B*), WPE1-NB14 malignant cells (*C*), WPE1-NB26 metastatic cells (*D*). Cells were plated at a density of 1 × 10^4 per well for 24 h, starved for 24 h, and treated with resveratrol at 24, 48, and 72 h. Subsequently, cells were treated with MTS for 1 h, measured at 490 nm, and plotted. *Columns,* mean absorbance; *bars,* SE. *, significant difference between resveratrol treatment and DMSO and untreated control.
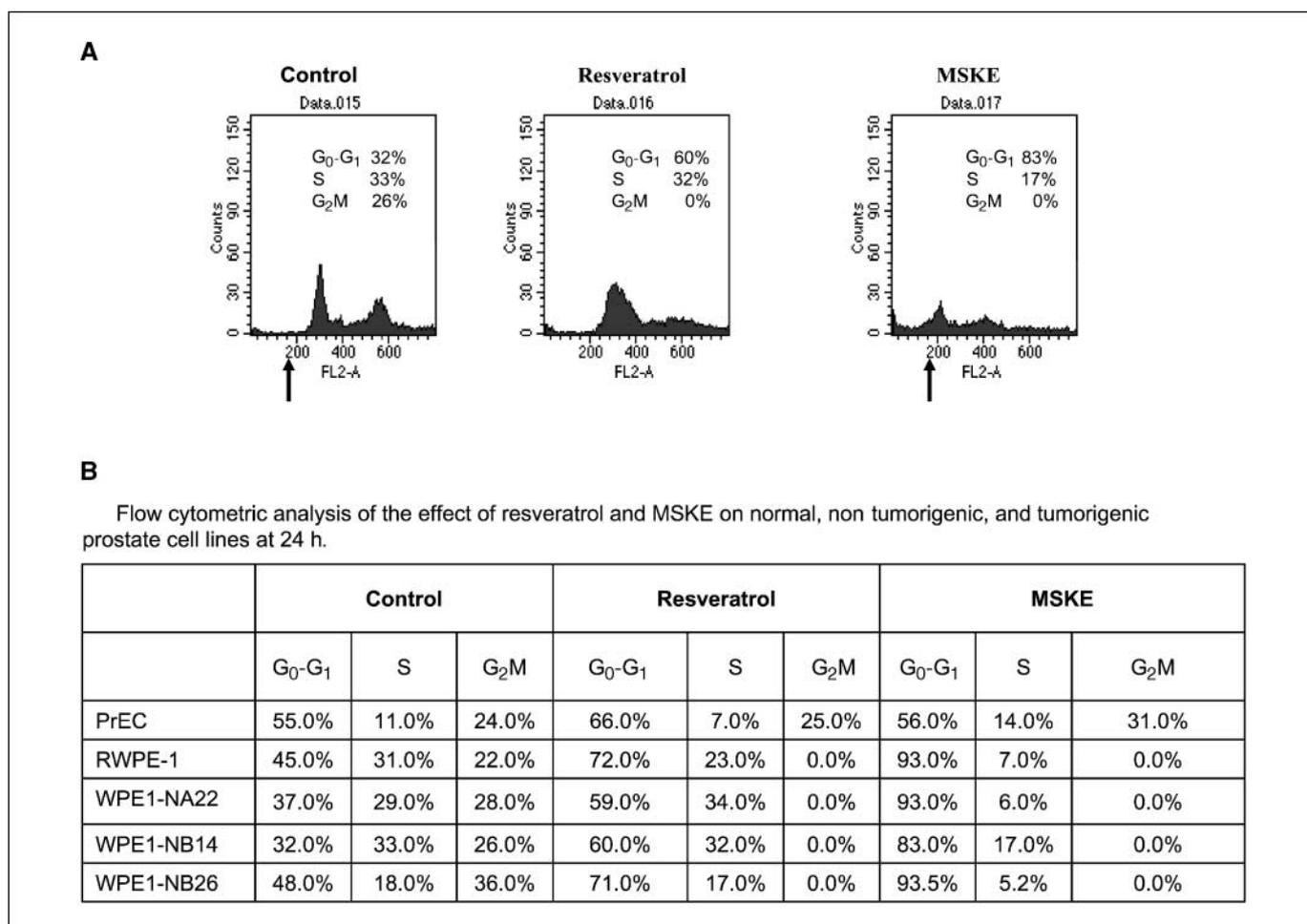
Figure 3. Resveratrol arrested cells in G_1-S phase transition in prostate cancer cells whereas GSE preferentially induced apoptosis. *A,* represents control, resveratrol, and MSKE treatment of WPE1-NB14 tumorigenic prostate cells. *B,* the flow cytometric analysis of normal, nontumorigenic, tumorigenic, and metastatic prostate cell lines untreated and treated with 25 μmol/L resveratrol and 20 μg/mL MSKE at 24 h. Cells were plated at a density of 1×10^5 per well in six-well plates in complete keratinocyte serum–free medium for 24 h. Subsequently, cells were synchronized for 24 h and then treated with resveratrol or MSKE. The cells were then harvested, fixed in ethanol, stained with propidium iodide, and analyzed by FACS. *Arrow* ($\uparrow$), position where apoptosis is likely occurring.

MSKE decreases Akt and DJ-1 mRNA expression levels. Treatment with MSKE reduced mRNA levels of all *Akt* isoforms and DJ-1, consistent with the results observed from the protein array and Western blot analyses. *Akt3* mRNA levels was reduced by at least 50% in WPE1-NA22 and WPE1-NB26 cells treated with MSKE for 8 h compared with untreated control cells (Supplementary Fig. S3*A*). Similarly, a 2-fold reduction in *DJ-1* mRNA levels was observed in WPE1-NB14 treated with MSKE compared with control cells. At least 2-fold reductions of mRNA levels were also observed for *Akt1, Akt2, Akt3,* and *DJ-1* mRNA levels in WPE1-NA22, WPE1-NB14, and WPE1-NB26 cells treated with MSKE at 24 h compared with untreated control cells (Supplementary Fig. S3*B*). However, a reduction in *Akt2* mRNA levels was not observed in WPE1-NB14 cells. Additional results indicate that *Akt1* and *Akt2* mRNA levels are significantly lower in the premalignant WPE1-NA22 cells compared with the metastatic WPE1-NB26 prostate cells by 8 h (Supplementary Fig. S3*A*). However, the difference was not maintained over time.

Discussion

The identification of new compounds with antitumor activities but minimal systemic toxicity is critical for discovering substances that may have significant effects in cancer prevention and possibly treatment. Some members of the flavonoid class of phytochemicals have been shown to inhibit tumorigenesis by numerous mechanisms, including antiinflammatory activities, induction of cell cycle arrest, inhibition of catalytic topoisomerase, suppression of cellular proliferation, stimulation of apoptosis and antioxidant properties (1). Because the effects of MSKE on prostate cancer have not been previously studied, we explored whether MSKE contains potentially novel compounds that can inhibit the growth of prostate cancer cells at different stages of tumor cell progression and through what mechanisms of action such antitumor activities are induced.

HPLC analyses showed that MSKE does not contain resveratrol, a compound commonly found in red grapes and red wines that exhibit many biological effects, including tumor inhibition. Additionally, chromatograms of MSKE show significant differences compared with chromatograms from muscadine seed extract, indicating that the skin and seed of the muscadine grape have very different chemical compositions with potentially unique biological properties. Preliminary purification analyses show that activity of MSKE can be segregated into subfractions which do not contain compounds with known antitumor activity including gallic acid, quercetin, and ellagic acid.
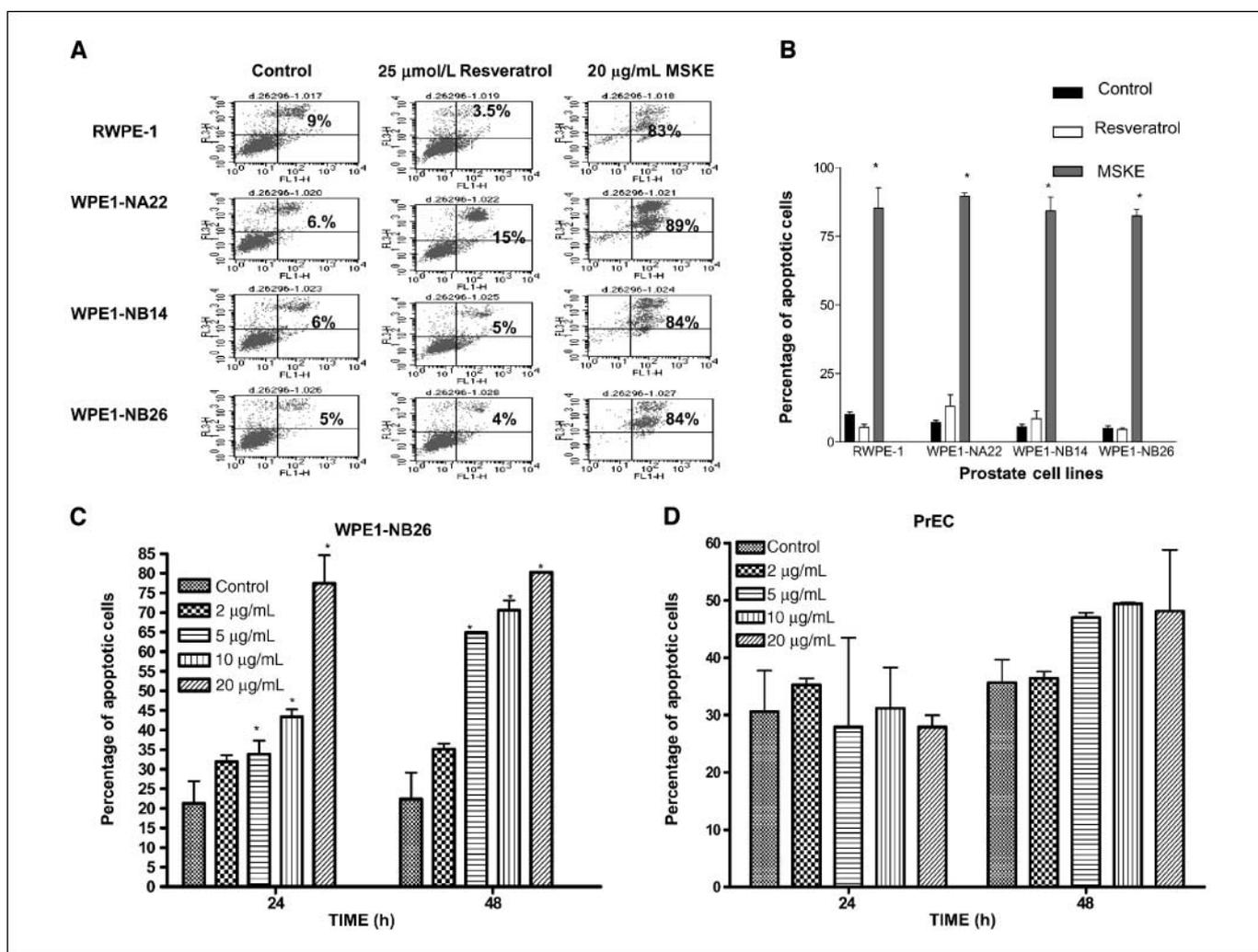
Figure 4. MSKE induces apoptosis in prostate cancer cells. *A,* MSKE induces apoptosis in RWPE-1, WPE1-NA22, WPE1-NB14, and WPE1-NB26 prostate cells. Cells were plated at a density of 1×10^5 per well for 24 h, starved for 24 h, and treated with resversrtol or MSKE. The cells were stained with Annexin V–FITC and analyzed by FACS. *B,* Annexin V–FITC. *Points,* percentage of apoptosis in a bar graph; *bars,* SE. *C,* MSKE induces apoptosis in a dose-dependent manner in treated WPE1-NB26 metastatic prostate cells. *D,* MSKE did not significantly induce apoptosis in treated PrEC normal cells. Annexin V–FITC. *Columns,* mean percentage of apoptosis; *bars,* SE. *, significant difference between treatment and control.

Because resveratrol has been previously studied in prostate cancer models (7, 23), we compared the effects of MSKE with that of resveratrol on a series of transformed human prostate cells, which include the RWPE-1 line (nontumorigenic), the WPE1-NB26 line (highly metastatic), and two cell lines with intermediate properties. Importantly, MSKE was found to exhibit different effects and mechanisms of action on the human cancer cells lines compared with resveratrol. Both MSKE and resveratrol did not alter the growth characteristics of normal human primary prostate epithelial cells, suggesting that these compounds may not induce toxic effects *in vivo*. Interestingly, the fact that all of the cell lines studied representing different stages of prostate cancer tumor progression responded to MSKE suggests that the active compound(s) in this extract may inhibit tumorigenesis at very early stages.

Distinct morphologic changes were observed in the MSKE and resveratrol treated tumor cells, but not normal primary cells. Changes in nuclear morphology and increased cell death suggested that MSKE was inducing apoptosis, whereas cells treated with resveratrol did not exhibit features of apoptosis and death. FACS analysis showed that treatment with resveratrol caused a G_1-S cell

cycle arrest, whereas treatment with MSKE induced a large fraction of cells in the sub-G_0 fraction consistent with apoptosis. Induction of apoptosis by MSKE was further confirmed by TUNEL assay. We further showed that MSKE exerted similar antitumor cell inhibitory action against the commonly studied LnCaP and DU-145 prostate cancer cell lines by inducing apoptosis. These data suggest that MSKE is targeting pathways involved in apoptosis and that resveratrol is targeting pathways involved in cell cycle arrest in this system. Therefore, MSKE and resveratrol seem to inhibit tumor growth in this model system through different mechanisms.

The PI3K, Akt, and MAPK have been shown to be critical regulators of prostate tumor growth through enhancing survival signaling and reducing apoptosis (24–26). The results of this study clearly show that MSKE increases JNK2, p38 isoforms (p38γ, p38α), and intracellular kinases (MSK2) and decreases intracellular kinases (ERK1, RSK1, Akt1, ERK2, GSK-3β, Akt3). The data suggest that MSKE is able to indirectly or directly target multiple pathways that are involved in cell survival and apoptosis. Previous studies have shown that the phytochemicals genstein and quercetin activate JNK and attenuate EGF, Akt1, and MAP/ERK kinase 1/2

in DU-145 and PC-3 metastatic prostate cancer cells (27, 28). In addition, Tyagi et al. showed that the induction of apoptosis in DU-145 prostate metastatic cells in response to grape seed extract is through the inhibition of EGF and activation of JNK (26). In this study, we show that the induction of apoptosis by MSKE may be induced in transformed, but nontumorigenic, prostate cells as well as in tumorigenic prostate cancer cells through the attenuation of the Akt pathway. The modulation of these important signaling proteins by MSKE was confirmed by Western blot analysis showing an increase in p38 and decreases in PI3K p85, phosphorylated PDK1, all three isoforms of Akt, phosphorylated Akt (Thr^{308}), phosphorylated ERK, phosphorylated p38, phosphorylated GSK-3β (Ser^9), cyclinD1, and androgen receptor at 30 min or 8 h.

DJ-1 is thought to be a critical regulator of the Akt pathway by negatively regulating PTEN (19, 29). For instance, it has been shown that reduced DJ-1 expression resulted in decreased phosphorylation of PI3K/Akt, whereas overexpression led to increased phosphorylation of PI3K and Akt and increased cell survival (29). Elevated levels of DJ-1 have been associated with human breast cancer (30). Although, DJ-1 was not modulated by MSKE at 8 h, DJ-1 protein

expression decreased at 24 h, suggesting that MSKE may indirectly target DJ-1. This is the first report suggesting that a phytochemical is capable of modulating DJ-1. Consistent with reduced protein expression of Akt and DJ-1 by MSKE, we observed a decrease in mRNA levels of all three *Akt* isoforms and *DJ-1* in WPE1-NA22, WPE1-NB14, and WPE1-NB26 prostate cancer cells.

Therefore, based on these results, we propose that MSKE may target different signaling pathways associated with cell proliferation and apoptotic cell death. MSKE targets the PI3K/Akt pathway by suppressing phosphorylation of the upstream effector molecule PI3K, thereby reducing activation of the survival kinase, Akt (protein kinase B). The decrease in total Akt and Akt phosphorylation results in decreased phosphorylation of GSK-3 and FKHR, and total cyclin D1 downstream effector molecules of the Akt survival pathway, leading to a decrease in cell survival and increased apoptosis.

MSKE action may also involve the p38 pathway, because MSKE induced phosphorylation (but not increased total levels) of p38 protein. In addition, we observed significant suppression of ERK1/ERK2 phosphorylation associated with decreased cell survival,
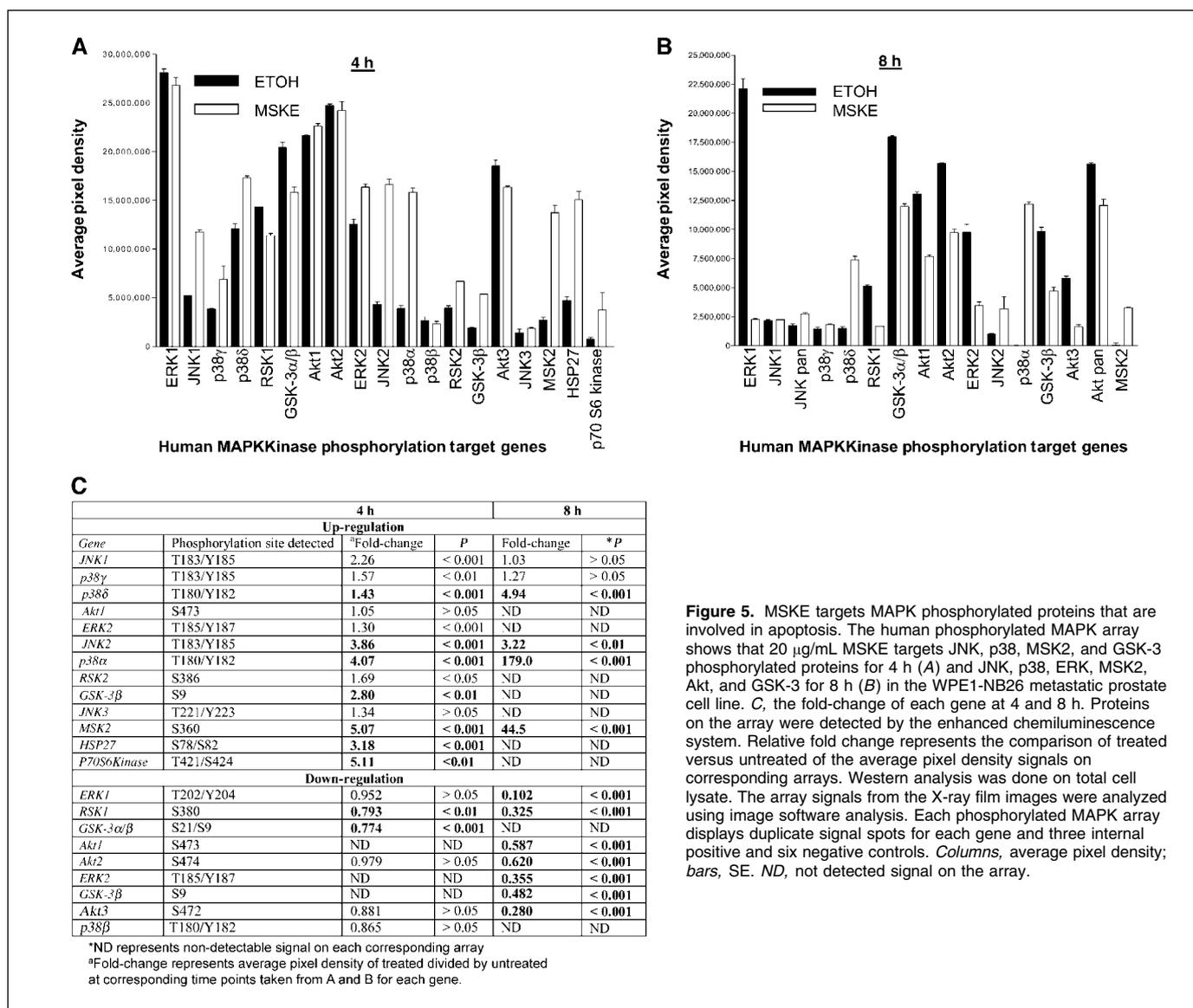

Figure 5. MSKE targets MAPK phosphorylated proteins that are involved in apoptosis. The human phosphorylated MAPK array shows that 20 μg/mL MSKE targets JNK, p38, MSK2, and GSK-3 phosphorylated proteins for 4 h (*A*) and JNK, p38, ERK, MSK2, Akt, and GSK-3 for 8 h (*B*) in the WPE1-NB26 metastatic prostate cell line. *C*, the fold-change of each gene at 4 and 8 h. Proteins on the array were detected by the enhanced chemiluminescence system. Relative fold change represents the comparison of treated versus untreated of the average pixel density signals on corresponding arrays. Western analysis was done on total cell lysate. The array signals from the X-ray film images were analyzed using image software analysis. Each phosphorylated MAPK array displays duplicate signal spots for each gene and three internal positive and six negative controls. *Columns,* average pixel density; *bars,* SE. *ND,* not detected signal on the array.

C

		4 h		8 h	
Gene	Phosphorylation site detected	^{a}Fold-change	*P*	Fold-change	**P*
Up-regulation					
JNK1	T183/Y185	2.26	< 0.001	1.03	> 0.05
p38γ	T183/Y185	1.57	< 0.01	1.27	> 0.05
p38δ	T180/Y182	**1.43**	**< 0.001**	**4.94**	**< 0.001**
Akt1	S473	1.05	> 0.05	ND	ND
ERK2	T185/Y187	1.30	< 0.001	ND	ND
JNK2	T183/Y185	**3.86**	**< 0.001**	**3.22**	**< 0.01**
p38α	T180/Y182	**4.07**	**< 0.001**	**179.0**	**< 0.001**
RSK2	S386	1.69	< 0.05	ND	ND
GSK-3β	S9	**2.80**	**< 0.01**	ND	ND
JNK3	T221/Y223	1.34	> 0.05	ND	ND
MSK2	S360	**5.07**	**< 0.001**	**44.5**	**< 0.001**
HSP27	S78/S82	**3.18**	**< 0.001**	ND	ND
P70S6Kinase	T421/S424	**5.11**	**<0.01**	ND	ND
Down-regulation					
ERK1	T202/Y204	0.952	> 0.05	**0.102**	**< 0.001**
RSK1	S380	**0.793**	**< 0.01**	**0.325**	**< 0.001**
GSK-3α/β	S21/S9	**0.774**	**< 0.001**	ND	ND
Akt1	S473	ND	ND	**0.587**	**< 0.001**
Akt2	S474	0.979	> 0.05	**0.620**	**< 0.001**
ERK2	T185/Y187	ND	ND	**0.355**	**< 0.001**
GSK-3β	S9	ND	ND	**0.482**	**< 0.001**
Akt3	S472	0.881	> 0.05	**0.280**	**< 0.001**
p38β	T180/Y182	0.865	> 0.05	ND	ND

*ND represents non-detectable signal on each corresponding array
^{a}Fold-change represents average pixel density of treated divided by untreated at corresponding time points taken from A and B for each gene.
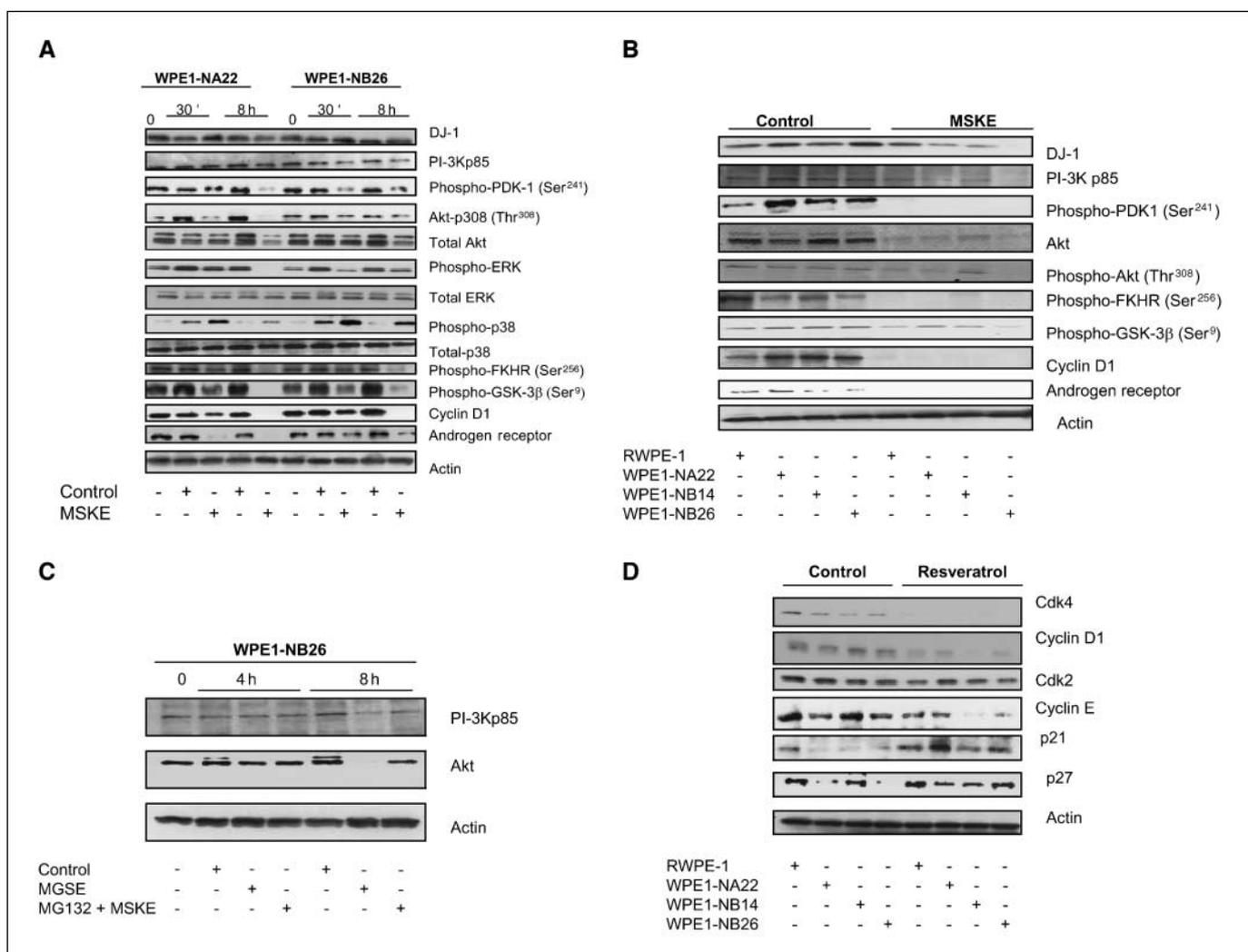
Figure 6. MSKE induces apoptosis through the PI3K/Akt cell survival pathway. *A,* WPE1-NA22 and WPE1-NB26 MSKE-treated cells were plated at a density of 6×10^5 per well for 24 h, starved for 24 h, and treated with or without 20 µg/mL MSKE for 0, 30, and 8 min. Western blot and immunodetection using anti-DJ-1, PI3k-p85, phosphorylated PDK1, AKT, phosphorylated Akt, ERK, phosphorylated ERK, p38, phosphorylated p38, phosphorylated GSK-3β, cyclin D1, and androgen receptor antibodies were done. *B,* Western blot and immunodetection using anti–DJ-1, PI3K-p85, phosphorylated PDK1, AKT, phosphorylated Akt, phosphorylated GSK-3β, cyclin D1, and androgen receptor antibodies were done in MSKE treated in RWPE-1, WPE1-NA22, WPE1-NB14, and WPE1-NB26 prostate cells for 24 h. *C,* 20 µg/mL MSKE induces degradation of Akt in prostate cancer cells. The WPE1-NB26 prostate cells were treated with 20 µg/mL MSKE or both MG132 and MSKE and the results reveal that MSKE causes degradation of Akt. *D,* 25 µmol/L Resveratrol induces cell cycle arrest through cell cycle regulators. The results reveal decreases in Cdk4, cyclin D1, Cdk2, and cyclin E and increases in p21, p27 protein expression in RWPE-1 nontumorigenic, WPE1-NA22 premalignant, WPE1-NB14 malignant, WPE1-NB26 metastatic prostate cells. All proteins were detected by the enhanced chemiluminescence system. All Western analyses were done on total cell lysate.

without changes in the total protein level of ERK1/ERK2. These results show that MSKE exerts potentially important antitumor activities through the effects on p38, ERK1/ERK2 and the PI3K/Akt pathways, potentially resulting in increase apoptosis. Future studies will elucidate more detailed mechanisms of action by MSKE on these signaling pathways.

An additional mechanism of action of MSKE on inhibition of the Akt survival pathway seems to involve increased proteosome-mediated degradation of Akt. The ubiquitin-proteosome degradation system plays a critical role in the degradation of cellular proteins that regulate cellular functions (31). When the metastatic WPE1-NB26 prostate cells were treated with MSKE, total Akt levels decreased compared with untreated cells. However, when these cells were treated with both MSKE and the proteosome inhibitor MG132, Akt protein levels did not decrease, suggesting that MSKE may target Akt for proteosome-mediated degradation of Akt.

Interestingly, resveratrol in this model system seemed to inhibit tumor cell growth through a different mechanism relative to MSKE, involving G_1-S phase cell cycle arrest. This was associated with a marked decrease in Cdk4 and cyclin D1 and a significant increase in the cell cycle inhibitor p21. In addition, we observed a decrease of cyclin E in the nontumorigenic, malignant, and metastatic prostate cell lines, in conjunction with an increase of p27 in nontumorigenic, and metastatic prostate cell lines. However, protein expression of cdk2, a cyclin-dependent kinase inhibitor of cyclin E, was not modulated by resveratrol in this model system. Thus, the data suggest that the primary targets of resveratrol in this model system possibly includes cdk4–cyclin D1 complex and p21. Our data are in agreement with other reported studies, which conclude that cdk4 and cyclin D1, p21, and p27 operate together as primary targets of resveratrol (32–35). Most importantly, these reports indicate that similar concentrations of resveratrol used in

the current study were responsible for the G_1-S phase arrest observed in the above studies.

Although previous reports also showed that concentrations of resveratrol (100–1,000 μmol/L) induced apoptosis, we did not observe a significant induction of apoptosis or senescence by resveratrol in the prostate cell model system used in this study when given at 100 μmol/L (data not shown). This suggests that resveratrol may preferentially activate different antitumor mechanisms, depending on the concentration used and the cell lines studied. However, the results presented in this study are the first to show that the cell cycle arrest induced by resveratrol can be induced in nontumorigenic prostate cell lines.

Although MSKE has significant inhibitory effects on the prostate cancer cell lines, it did not alter the growth variables of normal human primary prostate cells. This strongly suggests that the effects of MSKE may be specific for transformed cells, even at early stages, and that MSKE may be potentially very useful as a chemopreventive agent. Muscadine grape products, including grape juice (given 4 mL/kg twice daily for 14 days) and grape wine (given isocalorically at 240 mL/day) have been used in human studies without reported toxicities (36, 37), further suggesting that MSKE may be relatively safe in clinical trials. Therefore, MSKE may be useful as a chemopreventive or therapeutic agent. Ongoing *in vivo* studies of MSKE will further address the potential effects of MSKE in preventing or inhibiting prostate cancer growth.

Acknowledgments

References

1. Neuhouser ML. Dietary flavonoids and cancer risk: evidence from human population studies. Nutr Cancer 2004;50:1–7.
2. Harkonen PL, Makela SI. Role of estrogens in development of prostate cancer. J Steroid Biochem Mol Biol 2004;92:297–305.
3. Ozasa K, Nakao M, Watanabe Y, et al. Serum phytoestrogens and prostate cancer risk in a nested case-control study among Japanese men. Cancer Sci 2004;95:65–71.
4. Hammerschmidt R. PHYTOALEXINS: What Have We Learned After 60 Years? Annu Rev Phytopathol 1999;37: 285–306.
5. Pozo-Guisado E, Alvarez-Barrientos A, Mulero-Navarro S, Santiago-Josefat B, Fernandez-Salguero PM. The antiproliferative activity of resveratrol results in apoptosis in MCF-7 but not in MDA-MB-231 human breast cancer cells: cell-specific alteration of the cell cycle. Biochem Pharmacol 2002;64:1375–86.
6. Ding XZ, Adrian TE. Resveratrol inhibits proliferation and induces apoptosis in human pancreatic cancer cells. Pancreas 2002;25:e71–6.
7. Hsieh TC, Wu JM. Differential effects on growth, cell cycle arrest, and induction of apoptosis by resveratrol in human prostate cancer cell lines. Exp Cell Res 1999;249: 109–15.
8. Lee JH, Talcott ST. Ellagic acid and ellagitannins affect on sedimentation in muscadine juice and wine. J Agric Food Chem 2002;50:3971–6.
9. Heinonen IM, Lehtonen PJ, Hopia AI. Antioxidant Activity of Berry and Fruit Wines and Liquors. J Agric Food Chem 1998;46:25–31.
10. Ichikawa H, Ichiyanagi T, Xu B, Yoshii Y, Nakajima M, Konishi T. Antioxidant Activity of Anthocyanin Extract from Purple Black Rice. J Med Food 2001;4:211–8.
11. Jung KJ, Wallig MA, Singletary KW. Purple grape juice inhibits 7,12-dimethylbenz[a]anthracene (DMBA)-induced rat mammary tumorigenesis and *in vivo* DMBA-DNA adduct formation. Cancer Lett 2006;233:279–88.
12. Singletary KW, Stansbury MJ, Giusti M, Van Breemen RB, Wallig M, Rimando A. Inhibition of rat mammary tumorigenesis by concord grape juice constituents. J Agric Food Chem 2003;51:7280–6.
13. Bagchi D, Sen CK, Bagchi M, Atalay M. Antiangiogenic, antioxidant, and anti-carcinogenic properties of a novel anthocyanin-rich berry extract formula. Biochemistry (Mosc) 2004;69:75–80, 71 p preceding 75.
14. Tate P, God J, Bibb R, Lu Q, Larcom LL. Inhibition of metalloproteinase activity by fruit extracts. Cancer Lett 2004;212:153–8.
15. Agarwal C, Sharma Y, Agarwal R. Anticarcinogenic effect of a polyphenolic fraction isolated from grape seeds in human prostate carcinoma DU145 cells: modulation of mitogenic signaling and cell-cycle regulators and induction of G_1 arrest and apoptosis. Mol Carcinog 2000;28:129–38.
16. Webber MM, Quader ST, Kleinman HK, et al. Human cell lines as an *in vitro/in vivo* model for prostate carcinogenesis and progression. Prostate 2001;47:1–13.
17. Wurthner JU, Frank DB, Felici A, et al. Transforming growth factor-β receptor-associated protein 1 is a Smad4 chaperone. J Biol Chem 2001;276:19495–502.
18. Nakatani K, Thompson DA, Barthel A, et al. Up-regulation of Akt3 in estrogen receptor-deficient breast cancers and androgen-independent prostate cancer lines. J Biol Chem 1999;274:21528–32.
19. Kim RH, Peters M, Jang Y, et al. DJ-1, a novel regulator of the tumor suppressor PTEN. Cancer Cell 2005;7:263–73.
20. Alvarez E, Northwood IC, Gonzalez FA, et al. Pro-Leu-Ser/Thr-Pro is a consensus primary sequence for substrate protein phosphorylation. Characterization of the phosphorylation of c-myc and c-jun proteins by an epidermal growth factor receptor threonine 669 protein kinase. J Biol Chem 1991;266:15277–85.
21. Cobb MH, Goldsmith EJ. How MAP kinases are regulated. J Biol Chem 1995;270:14843–6.
22. Gonzalez FA, Raden DL, Davis RJ. Identification of substrate recognition determinants for human ERK1 and ERK2 protein kinases. J Biol Chem 1991;266:22159–63.
23. Kuwajerwala N, Cifuentes E, Gautam S, Menon M, Barrack ER, Reddy GP. Resveratrol induces prostate cancer cell entry into s phase and inhibits DNA synthesis. Cancer Res 2002;62:2488–92.
24. Ayala G, Thompson T, Yang G, et al. High levels of phosphorylated form of Akt-1 in prostate cancer and non-neoplastic prostate tissues are strong predictors of biochemical recurrence. Clin Cancer Res 2004;10:6572–8.
25. Thomas GV, Horvath S, Smith BL, et al. Antibody-based profiling of the phosphoinositide 3-kinase pathway in clinical prostate cancer. Clin Cancer Res 2004;10: 8351–6.
26. Tyagi A, Agarwal R, Agarwal C. Grape seed extract inhibits EGF-induced and constitutively active mitogenic signaling but activates JNK in human prostate carcinoma DU145 cells: possible role in antiproliferation and apoptosis. Oncogene 2003;22:1302–16.
27. Huynh H, Nguyen TT, Chan E, Tran E. Inhibition of ErbB-2 and ErbB-3 expression by quercetin prevents transforming growth factor α (TGF-α)- and epidermal growth factor (EGF)-induced human PC-3 prostate cancer cell proliferation. Int J Oncol 2003;23:821–9.
28. Li Y, Sarkar FH. Inhibition of nuclear factor κB activation in PC3 cells by genistein is mediated via Akt signaling pathway. Clin Cancer Res 2002;8:2369–77.
29. Yang Y, Gehrke S, Haque ME, et al. Inactivation of Drosophila DJ-1 leads to impairments of oxidative stress response and phosphatidylinositol 3-kinase/Akt signaling. Proc Natl Acad Sci U S A 2005;102:13670–5.
30. Le Naour F, Misek DE, Krause MC, et al. Proteomics-based identification of RS/DJ-1 as a novel circulating tumor antigen in breast cancer. Clin Cancer Res 2001;7: 3328–35.
31. Nam S, Smith DM, Dou QP. Ester bond-containing tea polyphenols potently inhibit proteasome activity *in vitro* and *in vivo*. J Biol Chem 2001;276:13322–30.
32. Ahmad N, Feyes DK, Nieminen AL, Agarwal R, Mukhtar H. Green tea constituent epigallocatechin-3-gallate and induction of apoptosis and cell cycle arrest in human carcinoma cells. J Natl Cancer Inst 1997;89: 1881–6.
33. Jacks T, Weinberg RA. Cell-cycle control and its watchman. Nature 1996;381:643–4.
34. Sherr CJ, Roberts JM. CDK inhibitors: positive and negative regulators of G_1-phase progression. Genes Dev 1999;13:1501–12.
35. Stadler WM, Vogelzang NJ, Amato R, et al. Flavopiridol, a novel cyclin-dependent kinase inhibitor, in metastatic renal cancer: a University of Chicago Phase II Consortium study. J Clin Oncol 2000;18:371–5.
36. Leighton F, Cuevas A, Guasch V, et al. Plasma polyphenols and antioxidants, oxidative DNA damage and endothelial function in a diet and wine intervention study in humans. Drugs Exp Clin Res 1999;25:133–41.
37. Stein JH, Keevil JG, Wiebe DA, Aeschlimann S, Folts JD. Purple grape juice improves endothelial function and reduces the susceptibility of LDL cholesterol to oxidation in patients with coronary artery disease. Circulation 1999;100:1050–5.

Inhibition of Prostate Cancer Growth by Muscadine Grape Skin Extract and Resveratrol through Distinct Mechanisms

Tamaro S. Hudson, Diane K. Hartle, Stephen D. Hursting, et al.

Updated version	Access the most recent version of this article at: http://cancerres.aacrjournals.org/content/67/17/8396
Supplementary Material	Access the most recent supplemental material at: http://cancerres.aacrjournals.org/content/suppl/2008/12/29/67.17.8396.DC1

Cited articles	This article cites 37 articles, 15 of which you can access for free at: http://cancerres.aacrjournals.org/content/67/17/8396.full#ref-list-1
Citing articles	This article has been cited by 7 HighWire-hosted articles. Access the articles at: http://cancerres.aacrjournals.org/content/67/17/8396.full#related-urls

E-mail alerts	Sign up to receive free email-alerts related to this article or journal.
Reprints and Subscriptions	To order reprints of this article or to subscribe to the journal, contact the AACR Publications Department at pubs@aacr.org.
Permissions	To request permission to re-use all or part of this article, use this link http://cancerres.aacrjournals.org/content/67/17/8396. Click on "Request Permissions" which will take you to the Copyright Clearance Center's (CCC) Rightslink site.